

Edge states, corner states, and flat bands in a two-dimensional \mathcal{PT} -symmetric system

Akira Yoshida, Yuria Otaki, Rimako Otaki, and Takahiro Fukui
Department of Physics, Ibaraki University, Mito 310-8512, Japan

(Dated: September 20, 2019)

We study corner states on a flat band in the square lattice. To this end, we introduce a two dimensional model including Su-Schrieffer-Heeger type bond alternation responsible for corner states as well as next-nearest neighbor hoppings yielding flat bands. The key symmetry of the model for corner states is space-time inversion (\mathcal{PT}) symmetry, which guarantees quantized Berry phases. This implies that edge states as well as corner states would show up if boundaries are introduced to the system. We also argue that an infinitesimal \mathcal{PT} symmetry-breaking perturbation could drive flat bands into flat Chern bands.

I. INTRODUCTION

Topological properties of gapped ground states for bulk systems could be unveiled by edge states if boundaries are introduced to those systems. This is called bulk-edge (boundary) correspondence [1], which is nowadays one of the fundamental concepts in condensed matter physics. Except for the quantum Hall effect (QHE) states [2, 3], bulk topological invariants in various classes of topological insulators [4–6] are not necessarily related with the observables such as the Hall conductance. Therefore, experiments on topological insulators are mainly based on the observation of gapless surface states [7–10].

The conventional bulk-edge correspondence is the relationship between d -dimensional bulk gapped ground states and their $d - 1$ dimensional surface gapless states. Recently, the bulk-edge correspondence has been extended to higher-order topological insulators (HOTI) [11–15] which have $d - D$ dimensional boundary states generically with $D > 1$. The HOTI have been studied extensively with a broad interest in, e.g., symmetry properties and classification [16–22], model construction [23–26], a field theoretical point of view [27], superconducting systems [28–30], interaction effects [31], Floquet systems [32, 33], etc. Among them, the HOTI on the breathing Kagome lattice [23] may be quite interesting, since the model shows a flat band as well. Here, flat band systems [34–38] have been attracting continuous interest, not only in magnetism [34–36], but also the fractional QHE [39–42], and superconductivity [43, 44], especially in twisted bilayer graphene [45–61], etc. Thus, it may be interesting to investigate more generic flat bands with edge and/or corner states to seek the possibilities of wider topological phases of matter. Such systems would offer a promising platform for studying the interplay among magnetism, superconductivity, and topological phenomena.

In this paper, we investigate a model with inversion (\mathcal{P}) symmetry as well as time-reversal (\mathcal{T}) symmetry, which is an extension of the two-dimensional Su-Schrieffer-Heeger (SSH) model in Refs. [12–14], including next-nearest neighbor (NNN) hoppings [37]. We first argue that topological invariants for a \mathcal{PT} -symmetric system are quantized Berry phases [62–76] (or polarizations) which could be also topological invariants characterizing the HOTI. Moreover, with fine-tuned parameters

for the NNN hoppings, the model allows flat bands. Therefore, we can realize systems in which gapped edge states, corner states and flat bands coexist. We show that the model introduced in this paper has edge states and corner states on a flat-band like the breathing Kagome lattice model [23]. The flat bands with corner states thus derived are near the critical point to flat Chern bands in the sense that the band-crossing with a dispersive band and infinitesimal symmetry-breaking perturbations could turn these (trivial) flat bands into flat Chern bands. To show this, we introduce a locally fluctuating magnetic flux breaking both \mathcal{T} and \mathcal{P} symmetries but preserving \mathcal{PT} symmetry. We show that by increasing a small \mathcal{PT} symmetry-breaking perturbation, quantized step-like polarizations are changed into winding polarizations. This is achieved by infinitesimal \mathcal{P} -breaking perturbations with \mathcal{T} invariance.

II. \mathcal{PT} SYMMETRY

We first argue quantized Berry phases for \mathcal{PT} -symmetric systems [62–65, 69, 74]. Let $H(\mathbf{k})$ be a Hamiltonian and $\psi(\mathbf{k})$ be the n -multiplet, $H(\mathbf{k})\psi(\mathbf{k}) = \psi(\mathbf{k})\mathcal{E}(\mathbf{k})$. \mathcal{PT} symmetry is described by

$$PTH(\mathbf{k})(PT)^{-1} = H(\mathbf{k}), \quad (1)$$

where $T = K$ stands for the complex conjugation, and $(PT)^2 = 1$. This symmetry imposes the constraint on the wave function such that $\psi(\mathbf{k}) = [PT\psi(\mathbf{k})]U(\mathbf{k}) = P\psi^*(\mathbf{k})U(\mathbf{k})$, where $U(\mathbf{k})$ is a certain $n \times n$ unitary matrix. Let $A_\mu(\mathbf{k}) \equiv \text{tr} \psi^\dagger(\mathbf{k})\partial_\mu\psi(\mathbf{k})$ be the $U(1)$ Berry connection, where $\partial_\mu = \partial_{k_\mu}$ is the partial derivative with respect to the momentum k_μ . Then, the constraint on the wave function yields the identity,

$$A_\mu(\mathbf{k}) = -A_\mu(\mathbf{k}) + \text{tr} U^\dagger(\mathbf{k})\partial_\mu U(\mathbf{k}). \quad (2)$$

This implies that the Berry connection is a pure gauge, and hence, the polarization defined by

$$p_x(k_y) \equiv \frac{1}{2\pi i} \int_{-\pi}^{\pi} A_x(\mathbf{k}) dk_x, \quad (3)$$

is quantized such that

$$p_x(k_y) = \frac{n_x(k_y)}{2} \mod 1, \quad (4)$$

where $n_x(k_y) \equiv \frac{1}{2\pi i} \int \text{tr} U^\dagger(\mathbf{k}) \partial_x U(\mathbf{k}) dk_x$ is the winding number generically dependent on k_y . Likewise, the polarization $p_y(k_x)$ is quantized as $p_y(k_x) = \frac{n_y(k_x)}{2} \bmod 1$. If the multiplet under consideration is isolated from other bands by finite direct gaps over the whole Brillouin zone, the integers n_μ ($\mu = x, y$) should be constant, and the set of polarizations (p_x, p_y) can serve as the topological invariant for \mathcal{PT} -symmetric systems. It follows from Eq. (2) that for isolated multiplet bands the Berry curvature vanishes and the multiplet has zero first Chern number.

Let us focus our attention next on one specific band among the multiplets. The band degeneracies of \mathcal{PT} -symmetric systems have codimension 2, implying that the 2D systems have at most Dirac-like point nodes. With such point nodes, the polarizations $(p_x(k_y), p_y(k_x))$ of the specific band have jump discontinuities at those nodes. These discontinuities give rise to δ -function like singularities to Berry curvature. As far as \mathcal{PT} symmetry is preserved, the charge of monopoles at point nodes is indistinguishable, because $p = 1/2 = -1/2$ modulo 1. However, infinitesimal \mathcal{PT} symmetry breaking perturbations enables us to observe the charge. If the total monopole charge behind the multiplet under consideration is finite, it yields a finite Chern number if \mathcal{PT} symmetry is broken. Therefore, flat bands in \mathcal{PT} -symmetric systems could be converted into flat Chern bands. Interestingly, this can be achieved by \mathcal{P} -symmetry-breaking (but \mathcal{T} -symmetry-preserving) perturbations.

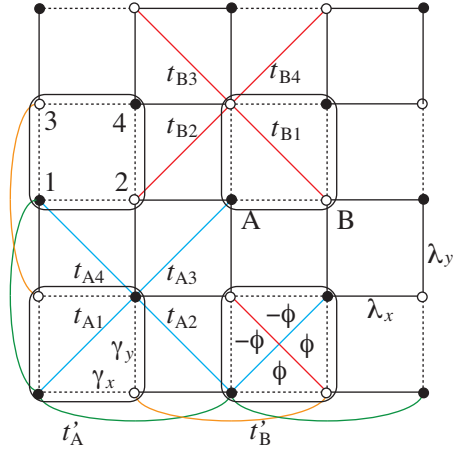


FIG. 1: Schematic illustration of the model defined in Eq. (5). γ_μ and λ_μ ($\mu = x, y$) are nearest neighbor hopping, denoting the SSH-like bond-alternating hoppings, whereas t_{aj} and t'_a ($a = A, B$ and $j = 1, \dots, 4$) are next-nearest neighbor hoppings necessary for flat bands. In a lower unit cell, we denote local flux ϕ which breaks \mathcal{T} and \mathcal{P} symmetries but preserves \mathcal{PT} symmetry.

III. MODEL

We now study the 2D version of the SSH model (Fig. 1) including next-nearest neighbor hoppings, $H(\mathbf{k}) = H_{\text{SSH}}(\mathbf{k}) + H_{\text{NNN}}(\mathbf{k})$, where H_{SSH} is the 2D generalization of the SSH model introduced in [12–14], and H_{NNN} is the next-nearest neighbor hopping terms necessary for flat bands [37]. They are given by

$$H_{\text{SSH}}(\mathbf{k}) = \begin{pmatrix} 0 & z_x^*(k_x) & z_y^*(k_y) & 0 \\ z_x(k_x) & 0 & 0 & z_y^*(k_y) \\ z_y(k_y) & 0 & 0 & z_x^*(k_x) \\ 0 & z_y(k_y) & z_x(k_x) & 0 \end{pmatrix},$$

$$H_{\text{NNN}}(\mathbf{k}) = \begin{pmatrix} d_A(\mathbf{k}) & 0 & 0 & z_A^*(\mathbf{k}) \\ 0 & d_B(\mathbf{k}) & z_B^*(\mathbf{k}) & 0 \\ 0 & z_B(\mathbf{k}) & d_B(\mathbf{k}) & 0 \\ z_A(\mathbf{k}) & 0 & 0 & d_A(\mathbf{k}) \end{pmatrix}, \quad (5)$$

where $z_\mu(k_\mu) \equiv \gamma_\mu + \lambda_\mu e^{ik_\mu}$ ($\mu = x, y$), $z_A(\mathbf{k}) = t_{A1} + t_{A2}e^{ik_x} + t_{A4}e^{ik_y} + t_{A3}e^{i(k_x+k_y)}$, $z_B(\mathbf{k}) = t_{B1} + t_{B2}e^{-ik_x} + t_{B4}e^{ik_y} + t_{B3}e^{i(-k_x+k_y)}$, and $d_a(\mathbf{k}) = 2t'_a(\cos k_x + \cos k_y)$ ($a = A, B$). For the time being, we assume that all the hopping parameters are real. Then, this model has \mathcal{T} symmetry and \mathcal{P} symmetry separately, where \mathcal{P} symmetry is implemented by $P = \sigma_1 \otimes \sigma_1$. Moreover, when $\gamma_x = \gamma_y$, $\lambda_x = \lambda_y$, $t_{Aj} = t_{Bj}$ ($j = 1, \dots, 4$), and $t'_A = t'_B$, $H(\mathbf{k})$ has C_4 symmetry. This model interpolates the 2D SSH model [12–14] and the flat band model [37]: The latter model is reproduced when $\gamma_\mu = \lambda_\mu$ for $\mu = x, y$ and $t'_a = t_{aj}/2$ for $a = A, B$ and $j = 1, \dots, 4$. For simplicity, we set $\lambda_x = \lambda_y = \lambda$ and $\gamma_x = \gamma_y \equiv \gamma$ in this paper. Thus, we assume C_4 symmetry in the basic H_{SSH} part. Then, based on the corner states of exactly solvable H_{SSH} , we will investigate the effect of H_{NNN} , which is responsible for flat bands.

A. Solvable decoupled model

Let us first review the model without H_{NNN} studied in Ref. [14]. The SSH part is exactly solvable, since $H_{\text{SSH}}(\mathbf{k}) = h_{\text{SSH}}(k_x) \otimes \mathbb{1} + \mathbb{1} \otimes h_{\text{SSH}}(k_y)$, where h_{SSH} is the conventional 1D SSH model [77]. Let $\psi_n(k)$ be the eigenstate of $h_{\text{SSH}}(k)$ such that $h_{\text{SSH}}(k)\psi_n(k) = \varepsilon_n(k)\psi_n(k)$, where $n = \pm$ stands for the positive and negative bands and $\varepsilon_n(k)$ ($\varepsilon_-(k) = -\varepsilon_+(k)$) is the energy eigenvalue. Clearly, the eigenstates and corresponding eigenvalues of $H_{\text{SSH}}(\mathbf{k})$ are given by $\psi_{nm}(\mathbf{k}) = \psi_n(k_x) \otimes \psi_m(k_y)$ and $\varepsilon_{nm}(\mathbf{k}) = \varepsilon_n(k_x) + \varepsilon_m(k_y)$, respectively. It follows that the present 2D model has four bands, one negative ε_{--} , one positive ε_{++} , and doubly-degenerate nearly zero-energy bands ε_{+-} and ε_{-+} . Each of these four bands has the polarizations $(p_x, p_y) = (1/2, 1/2)$ for $|\gamma/\lambda| < 1$ and $(0, 0)$ otherwise. Therefore, at 1/4- and 3/4-filling, the polarizations of the ground state are nontrivial when $|\gamma/\lambda| < 1$.

Such a decoupling property also holds for systems with boundaries. For the cylindrical system with an open

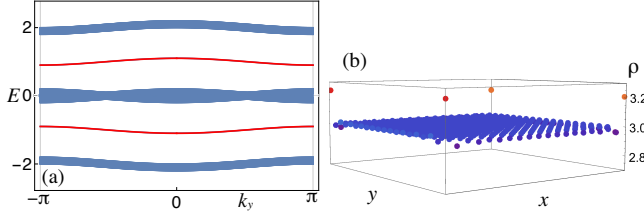


FIG. 2: (a) Energy spectrum of the cylindrical system with $\lambda = 1$ and $\gamma = 0.1$, in which edge states denoted by red lines can be observed. (b) Particle density at 3/4-filling.

boundary condition toward the x direction, the wave function of the 2D system is the tensor product of the wave function of the open SSH chain with respect to x and the wave function of the periodic SSH chain with respect to y , and the total spectrum is just given by the sum of corresponding energies. Therefore, it is obvious that in the case $|\gamma/\lambda| < 1$, the cylindrical system has gapped edge states, as shown in Fig. 2 (a), which are a combination of the Bloch states in the y direction and the edge states in the x direction. These edge states are themselves the 1D SSH states associated with $\psi_n(k_y)$, and their polarization is clearly $p_y = 1/2$. Therefore, for a full open system with four corners, the model shows corner states exactly at zero energy, even though they are embedded in the bulk spectrum. It thus turns out that the corner states are protected by the nontrivial polarizations (p_x, p_y) . In addition to the corner states, the model also has edge states, and since the Fermi energy lies within these edge states at 3/4- (1/4-) filling, there appear corner particle (hole) states affected by edge states [12–15]. Figure 2 (b) shows the particle density at 3/4-filling for the system in Fig. 2 (a) with full open boundary conditions imposed. One can see sharp peaks at four corners as well as the edge state contribution around the boundaries deviated slightly from the average density of the bulk.

B. Next-nearest neighbor hopping term and flat band

Let us next include next-nearest neighbor hoppings H_{NNN} to investigate flat bands with corner states. In the case of $\lambda = \gamma$, $t_{Aj} = t'_A/2$, and $t_{Bj} = t'_B = 0$, this model coincides with the model proposed in [37], implying that the Hamiltonian (5) has a complete flat band separated from a dispersive band by a finite gap. On the other hand, when $\lambda = 0$ or $\gamma = 0$ as well as $t_{Bj} = t'_B = 0$, one can prove that the model also has an exact flat band at zero energy for any other parameters t_{Aj} and t'_A . For simplicity, we restrict our model to

$$\begin{aligned} t_{Aj} &= 2t'_A = t_A \quad (j = 1, 2, 4), \quad t_{A3} = \epsilon_A t_A \\ t_{Bj} &= t'_B = 0. \end{aligned} \quad (6)$$

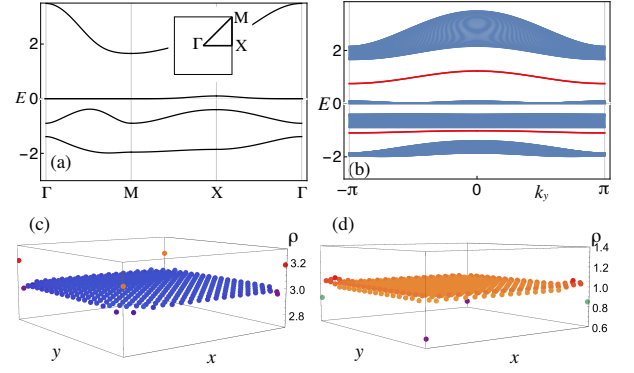


FIG. 3: (a) Spectrum of the bulk system. The inset shows the Brillouin zone. (b) Spectrum of the system with open boundary conditions toward the x direction. The edge states are highlighted by red lines. (c) and (d) Particle densities at 3/4- and 1/4-fillings, respectively. The parameters used are $\lambda = 1$, $\gamma = 0.1$, $t_A = 0.3$, and $\epsilon_A = 2$.

Figure 3 (a) shows the spectrum of the model with small $\gamma = 0.1$. The exact flat band when $\gamma = 0$ becomes slightly dispersive but is still an almost flat band. All four bands have the nontrivial polarizations $(1/2, 1/2)$. Therefore, the system with the open boundary condition toward, e.g., the x direction should have the edge states within the first gap and the third gap guaranteed by $p_x = 1/2$, as shown in Fig. 3 (b). Moreover, the nontrivial polarization $p_y = 1/2$ suggests that these edge states would form corner states around zero energy if we further impose the open boundary condition toward the y direction.

Indeed, the spectrum in Fig. 3 (b) can be obtained by an adiabatic deformation of the spectrum in Fig. 2 (c), implying that the edge states in both figures have the same topological property. Namely, those in Fig. 3 (b) have also polarization $p_y = 1/2$, and they are 1D topological insulators. Thus, for a full open system, corner states should emerge in between those edge states, probably around zero energy. We show in Figs. 3 (c) and (d) the particle density for a system with full open boundary condition at 3/4- and 1/4-filling, respectively. One can observe particle-like and hole-like densities at four corners, which are due to fully occupied and fully unoccupied corner states. A slight effect of the edge states can also be seen, since the Fermi energy is just on the edge states.

These edge and corner states are in sharp contrast to the trivial case, particularly, for the system with replaced parameters $\lambda \leftrightarrow \gamma$ (and also $t_{A1} \leftrightarrow t_{A3}$) which has the same bulk spectrum by definition. In this system, the polarizations of each band is $(0,0)$, and therefore, there are no edge states for a cylindrical system, as shown in Fig. 4 (a). Correspondingly, the corner states vanish as in Fig. 4 (b) for a full open system.

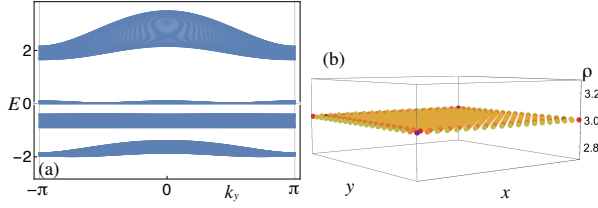


FIG. 4: (a) Spectrum of the system with open boundary conditions toward the x direction. (b) Particle density at $3/4$ -filling. The parameters used are replaced by $\lambda \leftrightarrow \gamma$, $t_{A1} \leftrightarrow t_{A3}$ in Fig. 3.

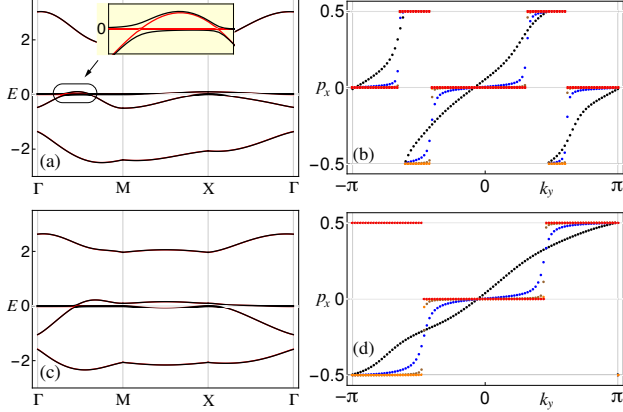


FIG. 5: (a) Spectrum with a flat band with a symmetry breaking potential. The red (black) lines show the spectrum with $v_{sb} = 0$ (0.1). Inset shows the gap formation near the point nodes. The other parameters are $\gamma = 0.1e^{i\phi}$ with $\phi = \pi/2$, $t_A = 0.3$, and $\epsilon_A = 2/3$. (b) Polarization $p_x(k_y)$ of the flat (third) band. The red, orange, brown, blue, black dots are the cases with $v_{sb} = 0, 10^{-4}, 10^{-3}, 10^{-2}, 10^{-1}$, respectively. (c) Spectrum and (d) the polarization $p_x(k_y)$ for the same system as (a) and (b) except for the $t'_A = 0$.

C. \mathcal{PT} symmetry breaking and flat Chern band

So far we have discussed the edge and corner states of the nearly flat band with nontrivial polarizations $(p_x, p_y) = (1/2, 1/2)$. The quantization of these polarizations is due to \mathcal{PT} symmetry, which also ensures vanishing Berry curvatures and Chern numbers. We next consider the possibility of converting such a flat band into a flat Chern band. First, band inversions with dispersive bands may be necessary. For the present model, this can be controlled by the parameter ϵ_A in Eq. (6). Second, \mathcal{T} symmetry should be broken. To this end, let us introduce locally fluctuating magnetic flux with zero mean [78], as denoted in Fig. 1. It can be incorporated simply by replacing γ_μ with $\gamma_\mu \rightarrow \gamma_\mu e^{i\phi}$ for $\mu = x, y$. Such flux ϕ breaks not only \mathcal{T} symmetry but also \mathcal{P} symmetry. Nevertheless, \mathcal{PT} symmetry is preserved, implying that the flat band is still a trivial Chern band. In Fig. 5, we show the spectrum (red lines in (a)) and the polar-

ization $p_x(k_y)$ (red dots in (b)) of the flat band for systems with \mathcal{PT} symmetry only, including finite local flux ϕ . The quantized polarization $p_x(k_y)$ of the flat band due to \mathcal{PT} symmetry has several jump discontinuities. These are a hallmark of Dirac-like level-crossings, which indeed occur as point nodes because of the codimension 2 of \mathcal{PT} -symmetric systems. These point nodes give rise to singular Berry curvature. Finally, if \mathcal{PT} symmetry-breaking perturbations are introduced, gaps are formed at these point nodes, and discontinuities of the polarization could become smoothly winding between $k_\mu = -\pi$ and π . The winding number of the polarization is merely the Chern number, and thus, a trivial flat band would be converted into a flat Chern band. To show this, we introduce \mathcal{P} -symmetry breaking potentials to the Hamiltonian

$$H_{\text{on}} = v_{\text{sb}} \sigma_3 \otimes \mathbb{1} + v'_{\text{sb}} \mathbb{1} \otimes \sigma_3. \quad (7)$$

These real onsite potentials of course preserve \mathcal{T} symmetry, but they break \mathcal{PT} symmetry. Below, we take only the v_{sb} term into account in Eq. (7), setting $v'_{\text{sb}} = 0$, for simplicity. In Fig. 5 (a), we show the spectrum of the system with a small \mathcal{P} symmetry breaking potential (black lines). One can observe that small gaps are indeed formed at the point nodes. As can be seen from the polarization $p_x(k_y)$ of the flat band denoted by black points in Fig. 5 (b), the winding number of p_x is 2, implying the Chern number -2 . The direct computation of Chern numbers [79] also supports this result. In this figure, one also sees how the step-like function of the polarization for a \mathcal{PT} symmetric system changes into a function with a winding number, when one varies the symmetry-breaking potential. Basically, for infinitesimal perturbations, the flat band becomes a flat Chern band. In this sense, the present \mathcal{PT} symmetric flat band is just on the critical point from a trivial band to a Chern band. Another example is shown in Fig. 5 (c) and (d) which is the same model as in (a) and (b) except for $t'_A = 0$. The winding number of the polarization implies the Chern number -1 .

IV. SUMMARY AND DISCUSSIONS

In summary, we have studied a \mathcal{PT} symmetric system having a flat band together with edge and corner states due to nontrivial polarizations. We have argued that the flat band of the model could be changed into a flat Chern band by symmetry-breaking perturbations. For flat band superconductors, the intersection of flat bands and dispersive bands is important [37, 43, 44]. Thus, it may be interesting to consider the possibility of flat band superconductors with edge and/or corner states, especially paying attention to the role played by those states. As argued in [21], C_n group allows various fractional charges at corners. It may thus be interesting to consider the interplay between flat bands and edge and/or corner states in systems with more generic point group symmetry [21, 80].

We also note that without C_4 symmetry, H_{SSH} Hamiltonian has unusual corner states inherent to 2D nature of the model [81]. It may be quite interesting to study such a model including H_{NNN} .

We would like to thank H. Aoki for fruitful discussions. This work was supported in part by Grants-in-Aid for Scientific Research Numbers 17K05563 and 17H06138 from the Japan Society for the Promotion of Science.

-
- [1] Y. Hatsugai, Physical Review Letters **71**, 3697 (1993).
 - [2] D. J. Thouless, M. Kohmoto, M. P. Nightingale, and M. den Nijs, Physical Review Letters **49**, 405 (1982).
 - [3] M. Kohmoto, Annals of Physics **160**, 343 (1985).
 - [4] C. L. Kane and E. J. Mele, Physical Review Letters **95**, 146802 (2005).
 - [5] X.-L. Qi, T. L. Hughes, and S.-C. Zhang, Physical Review B **78**, 195424 (2008).
 - [6] A. P. Schnyder, S. Ryu, A. Furusaki, and A. W. W. Ludwig, Physical Review B **78**, 195125 (2008).
 - [7] M. König, H. Buhmann, L. W. Molenkamp, T. Hughes, C.-X. Liu, X.-L. Qi, and S.-C. Zhang, J. Phys. Soc. Jpn. **77**, 031007 (2008).
 - [8] M. Z. Hasan and C. L. Kane, Reviews of Modern Physics **82**, 3045 (2010).
 - [9] X.-L. Qi and S.-C. Zhang, Reviews of Modern Physics **83**, 1057 (2011).
 - [10] Y. Ando, Journal of the Physical Society of Japan **82**, 102001 (2013).
 - [11] R.-J. Slager, L. Rademaker, J. Zaanen, and L. Balents, Physical Review B **92**, 085126 (2015).
 - [12] W. A. Benalcazar, B. A. Bernevig, and T. L. Hughes, Physical Review B **96**, 245115 (2017).
 - [13] W. A. Benalcazar, B. A. Bernevig, and T. L. Hughes, Science **357**, 61 (2017).
 - [14] F. Liu and K. Wakabayashi, Physical Review Letters **118**, 076803 (2017).
 - [15] F. Schindler, A. M. Cook, M. G. Vergniory, Z. Wang, S. S. P. Parkin, B. A. Bernevig, and T. Neupert, Science Advances **4**, eaat0346 (2018).
 - [16] J. Langbehn, Y. Peng, L. Trifunovic, F. von Oppen, and P. W. Brouwer, Physical Review Letters **119**, 246401 (2017).
 - [17] Z. Song, Z. Fang, and C. Fang, Physical Review Letters **119**, 246402 (2017).
 - [18] E. Khalaf, Physical Review B **97**, 205136 (2018).
 - [19] T. Fukui and Y. Hatsugai, Physical Review B **98**, 035147 (2018).
 - [20] L. Trifunovic and P. W. Brouwer, Physical Review X **9**, 011012 (2019).
 - [21] W. A. Benalcazar, T. Li, and T. L. Hughes, Physical Review B **99**, 245151 (2019).
 - [22] A. Matsugatani and H. Watanabe, Physical Review B **98**, 205129 (2018).
 - [23] M. Ezawa, Physical Review Letters **120**, 026801 (2018).
 - [24] M. Ezawa, Physical Review B **98**, 045125 (2018).
 - [25] D. Čalugăru, V. Juričić, and B. Roy, Physical Review B **99**, 041301 (2019).
 - [26] M. Ezawa, Physical Review B **98**, 201402 (2018).
 - [27] K. Hashimoto, X. Wu, and T. Kimura, Physical Review B **95**, 165443 (2017).
 - [28] Y. Wang, M. Lin, and T. L. Hughes, Physical Review B **98**, 165144 (2018).
 - [29] C.-H. Hsu, P. Stano, J. Klinovaja, and D. Loss, Physical Review Letters **121**, 196801 (2018).
 - [30] S. A. A. Ghorashi, X. Hu, T. L. Hughes, and E. Rossi, Physical Review B **100**, 020509 (2019).
 - [31] Y. You, T. Devakul, F. J. Burnell, and T. Neupert, Physical Review B **98**, 235102 (2018).
 - [32] R. W. Bomantara, L. Zhou, J. Pan, and J. Gong, Physical Review B **99**, 045441 (2019).
 - [33] M. Rodriguez-Vega, A. Kumar, and B. Seradjeh (2018), arXiv:1811.04808.
 - [34] E. H. Lieb, Physical Review Letters **62**, 1201 (1989).
 - [35] A. Mielke, **24**, L73 (1991).
 - [36] H. Tasaki, Physical Review Letters **69**, 1608 (1992).
 - [37] T. Misumi and H. Aoki, Physical Review B **96**, 155137 (2017).
 - [38] J.-W. Rhim and B.-J. Yang, Physical Review B **99**, 045107 (2019).
 - [39] K. Sun, Z. Gu, H. Katsura, and S. Das Sarma, Physical Review Letters **106**, 236803 (2011).
 - [40] E. Tang, J.-W. Mei, and X.-G. Wen, Physical Review Letters **106**, 236802 (2011).
 - [41] T. Neupert, L. Santos, C. Chamon, and C. Mudry, Physical Review Letters **106**, 236804 (2011).
 - [42] S. Yang, Z.-C. Gu, K. Sun, and S. Das Sarma, Physical Review B **86**, 241112 (2012).
 - [43] K. Kobayashi, M. Okumura, S. Yamada, M. Machida, and H. Aoki, Physical Review B **94**, 214501 (2016).
 - [44] M. Tovmasyan, S. Peotta, P. Törmä, and S. D. Huber, Physical Review B **94**, 245149 (2016).
 - [45] Y. Cao, V. Fatemi, S. Fang, K. Watanabe, T. Taniguchi, E. Kaxiras, and P. Jarillo-Herrero, Nature **556**, 43 EP (2018).
 - [46] V. Fatemi, S. Wu, Y. Cao, L. Bretheau, Q. D. Gibson, K. Watanabe, T. Taniguchi, R. J. Cava, and P. Jarillo-Herrero, Science **362**, 926 (2018).
 - [47] L. Zou, H. C. Po, A. Vishwanath, and T. Senthil, Physical Review B **98**, 085435 (2018).
 - [48] L. Rademaker and P. Mellado, Physical Review B **98**, 235158 (2018).
 - [49] J. W. F. Venderbos and R. M. Fernandes, Physical Review B **98**, 245103 (2018).
 - [50] A. Ramires and J. L. Lado, Physical Review Letters **121**, 146801 (2018).
 - [51] M. Koshino, N. F. Q. Yuan, T. Koretsune, M. Ochi, K. Kuroki, and L. Fu, Physical Review X **8**, 031087 (2018).
 - [52] T. J. Peltonen, R. Ojajärvi, and T. T. Heikkilä, Physical Review B **98**, 220504 (2018).
 - [53] H. C. Po, L. Zou, A. Vishwanath, and T. Senthil, Physical Review X **8**, 031089 (2018).
 - [54] H. Guo, X. Zhu, S. Feng, and R. T. Scalettar, Physical Review B **97**, 235453 (2018).
 - [55] M. Ochi, M. Koshino, and K. Kuroki, Physical Review B **98**, 081102 (2018).
 - [56] X. Lin, D. Liu, and D. Tománek, Physical Review B **98**, 195432 (2018).
 - [57] D. M. Kennes, J. Lischner, and C. Karrasch, Physical

- Review B **98**, 241407 (2018).
- [58] Y. W. Choi and H. J. Choi, Physical Review B **98**, 241412 (2018).
 - [59] J.-B. Qiao, L.-J. Yin, and L. He, Physical Review B **98**, 235402 (2018).
 - [60] K. Hejazi, C. Liu, H. Shapourian, X. Chen, and L. Balents, Physical Review B **99**, 035111 (2019).
 - [61] G. Tarnopolsky, A. J. Kruchkov, and A. Vishwanath, Physical Review Letters **122**, 106405 (2019).
 - [62] R. Yu, H. Weng, Z. Fang, X. Dai, and X. Hu, Physical Review Letters **115**, 036807 (2015).
 - [63] Y. Kim, B. J. Wieder, C. L. Kane, and A. M. Rappe, Physical Review Letters **115**, 036806 (2015).
 - [64] H. Huang, J. Liu, D. Vanderbilt, and W. Duan, Physical Review B **93**, 201114 (2016).
 - [65] D.-W. Zhang, Y. X. Zhao, R.-B. Liu, Z.-Y. Xue, S.-L. Zhu, and Z. D. Wang, Physical Review A **93**, 043617 (2016).
 - [66] Y. H. Chan, C.-K. Chiu, M. Y. Chou, and A. P. Schnyder, Physical Review B **93**, 205132 (2016).
 - [67] B. Pal and K. Saha, Physical Review B **97**, 195101 (2018).
 - [68] B. Pal, Physical Review B **98**, 245116 (2018).
 - [69] S. Li, Y. Liu, B. Fu, Z.-M. Yu, S. A. Yang, and Y. Yao, Physical Review B **97**, 245148 (2018).
 - [70] J. Ahn, D. Kim, Y. Kim, and B.-J. Yang, Physical Review Letters **121**, 106403 (2018).
 - [71] Z. Wang, B. J. Wieder, J. Li, B. Yan, and B. A. Bernevig (2018), arXiv:1806.11116.
 - [72] J. Ahn, S. Park, and B.-J. Yang (2018), arXiv:1808.05375.
 - [73] B. J. Wieder and B. A. Bernevig (2018), arXiv:1810.02373.
 - [74] C. K. Chiu, Y. H. Chan, and A. P. Schnyder (2018), arXiv:1810.04094.
 - [75] J. Ahn and B.-J. Yang, Physical Review B **99**, 235125 (2019).
 - [76] A. Ghatak and T. Das, Journal of Physics: Condensed Matter **31**, 263001 (2019).
 - [77] W. P. Su, J. R. Schrieffer, and A. J. Heeger, Physical Review Letters **42**, 1698 (1979).
 - [78] F. D. M. Haldane, Physical Review Letters **61**, 2015 (1988).
 - [79] T. Fukui, Y. Hatsugai, and H. Suzuki, Journal of the Physical Society of Japan **74**, 1674 (2005).
 - [80] C. Fang, M. J. Gilbert, and B. A. Bernevig, Physical Review B **86**, 115112 (2012).
 - [81] L. Li, M. Umer, and J. Gong, Physical Review B **98**, 205422 (2018).